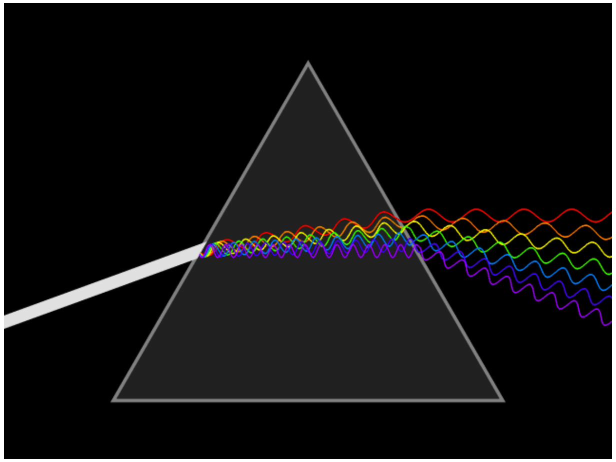

Spectral Dispersion and FLUOR

Nic Scott

Adapting FLUOR to CHARA

- Software updates to match current CHARA standards
- Ability to connect to other CHARA systems and instruments
- Remote observing

- Improve and add new systems

Ways to improve

- Fringe tracking (CHAMP)
  - Gives phase stability
  - Reduces piston error

Stabilizes OPD
Increased integration time
Increased sensitivity

- Spectral dispersion
  - Relative measures
  - Insensitive to Piston

More observables
and
New ways to observe

FLUOR layout

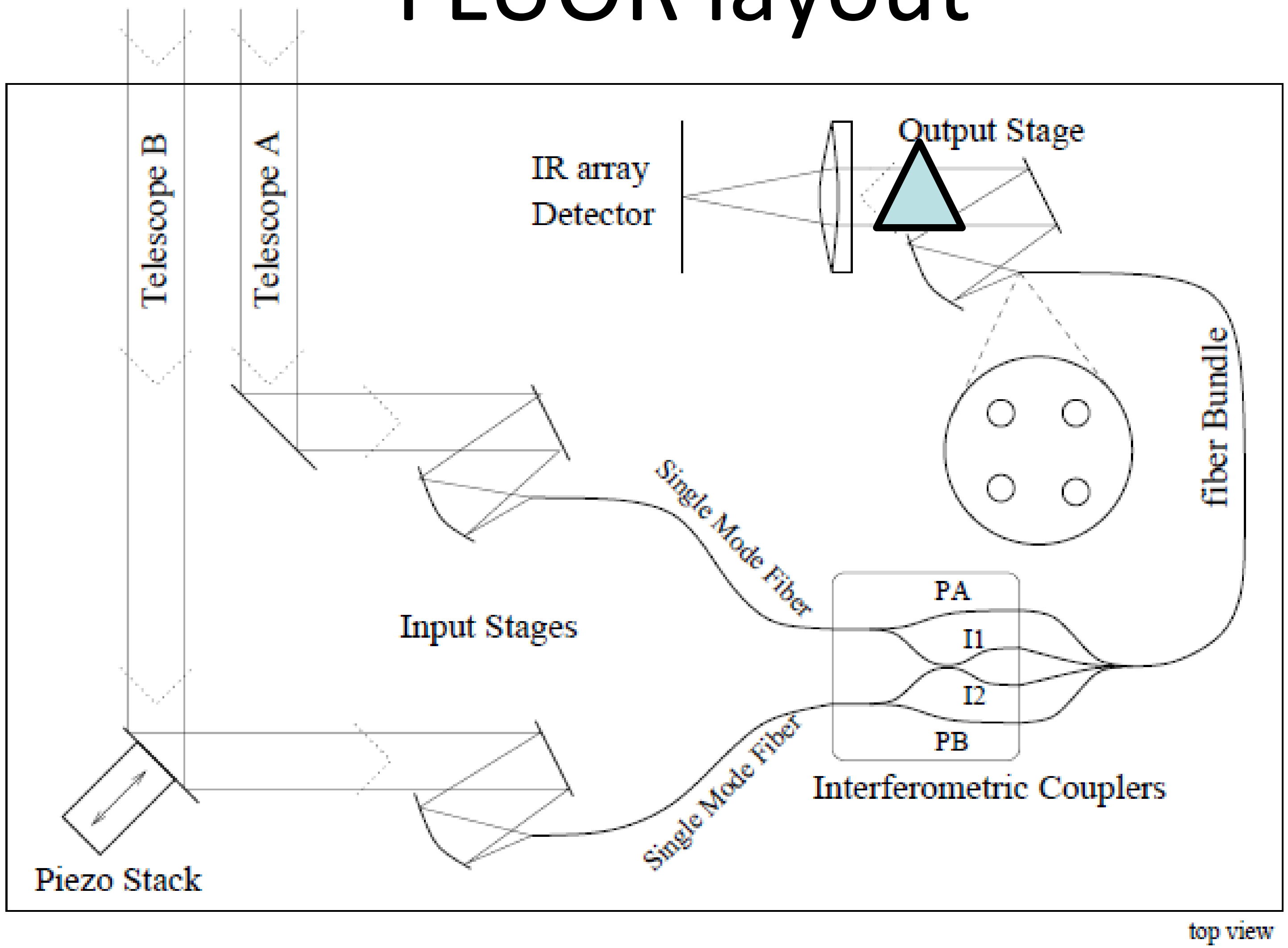

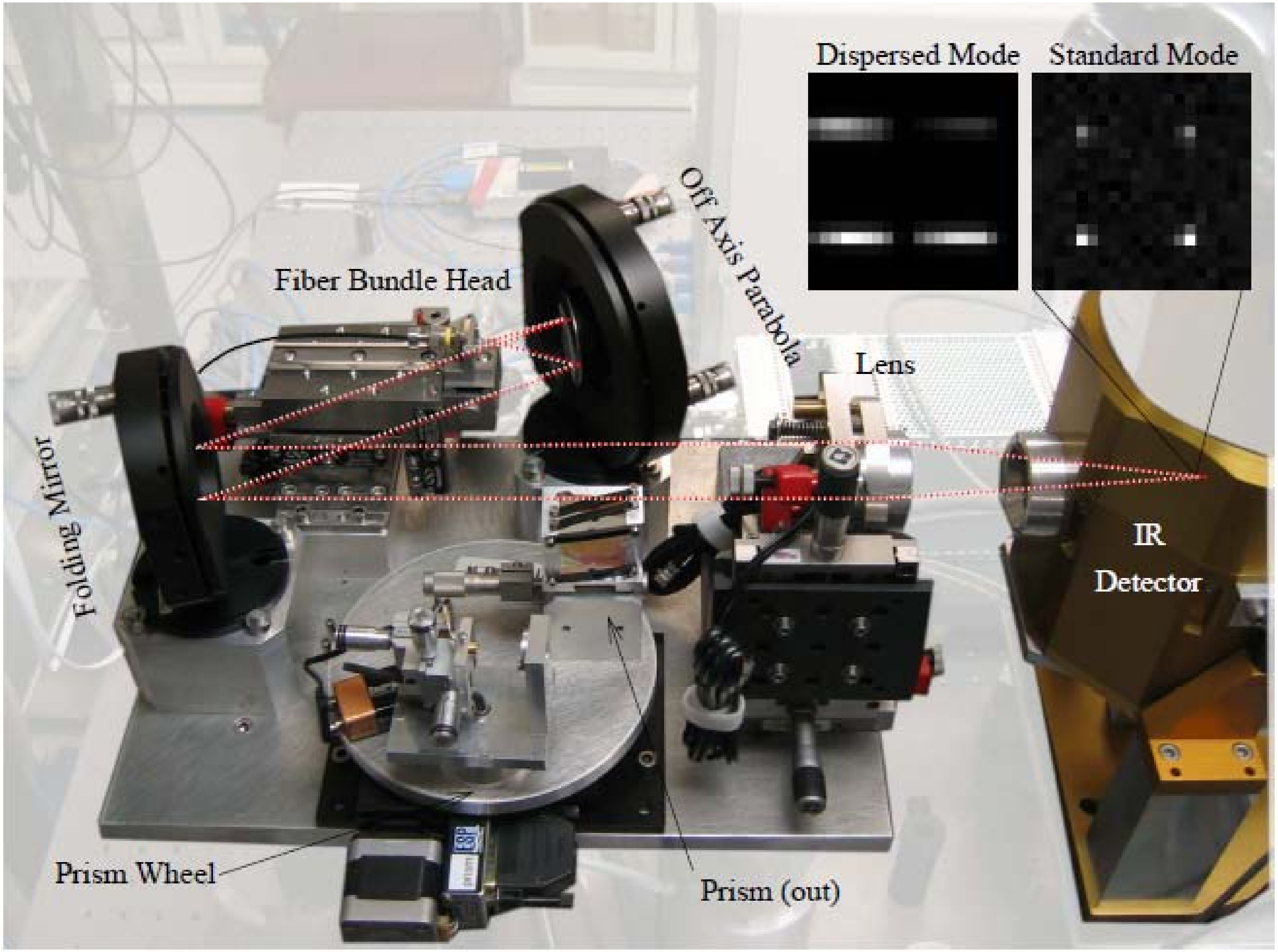
Dispersed Mode
Standard Mode
Off Axis Parabola
Fiber Bundle Head
Lens
Folding Mirror
IR
Detector
Prism Wheel
Prism (out)

Overlap

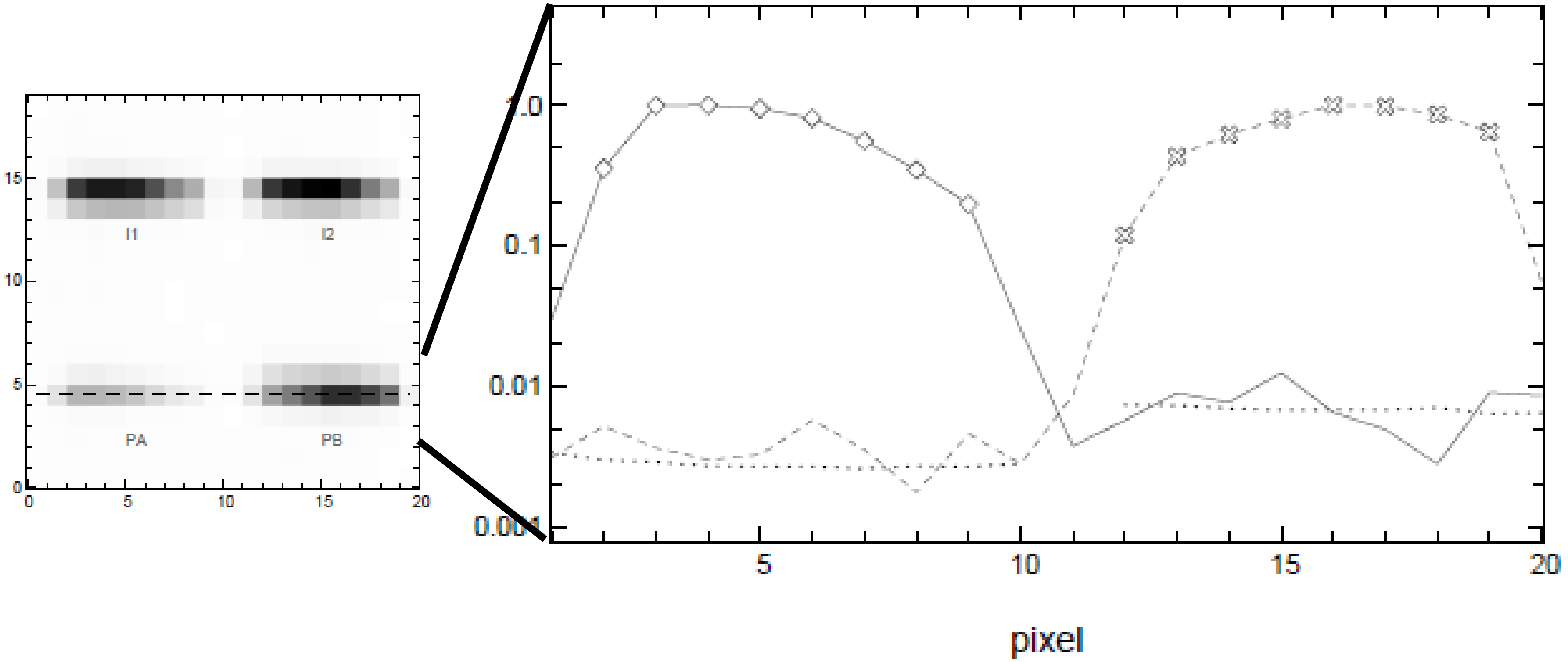

Advantages of dispersing light

- Resolve bandwidth smearing effect
- More spectral channels => more data
- Differential data
- Data 5x faster
- Detect slightly different angular resolutions

Resolve bandwidth smearing effect

- Ex. calibrator and target of different spectral type
- Increases accuracy of data

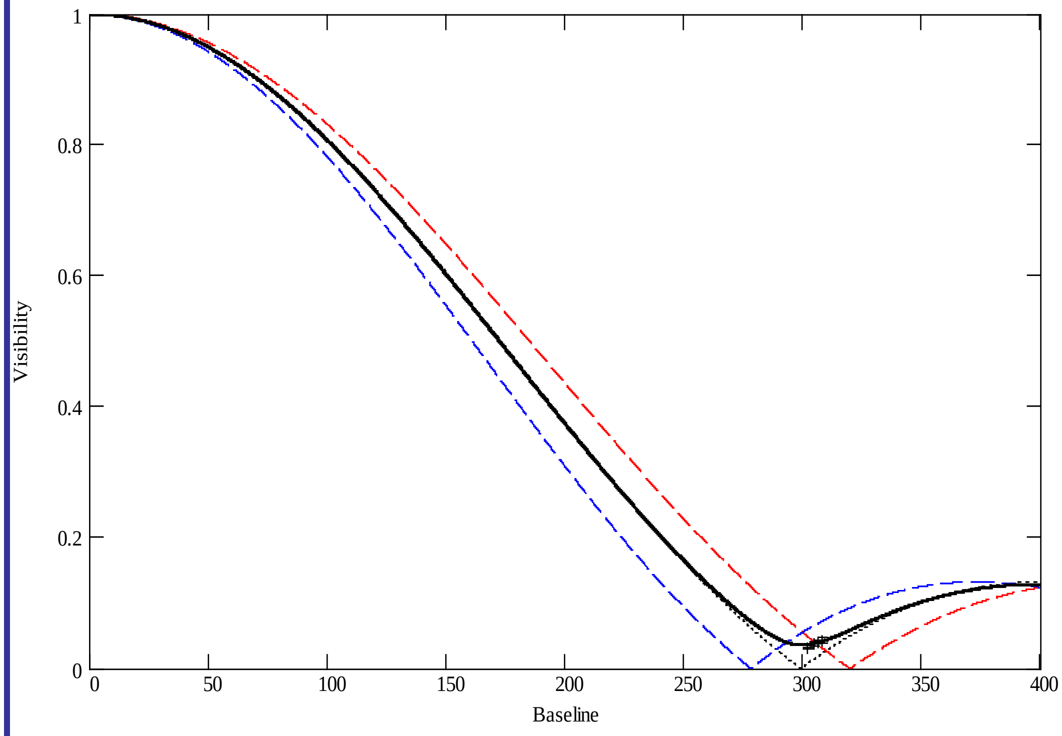

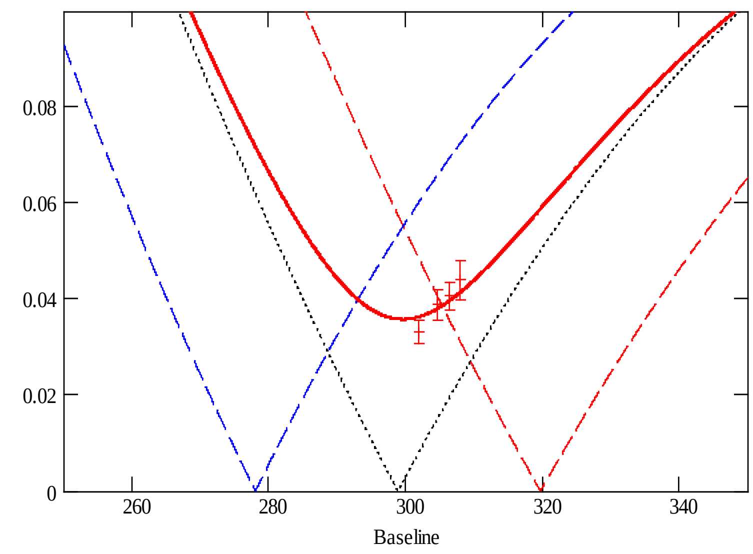

More spectral channels ⟹ more data

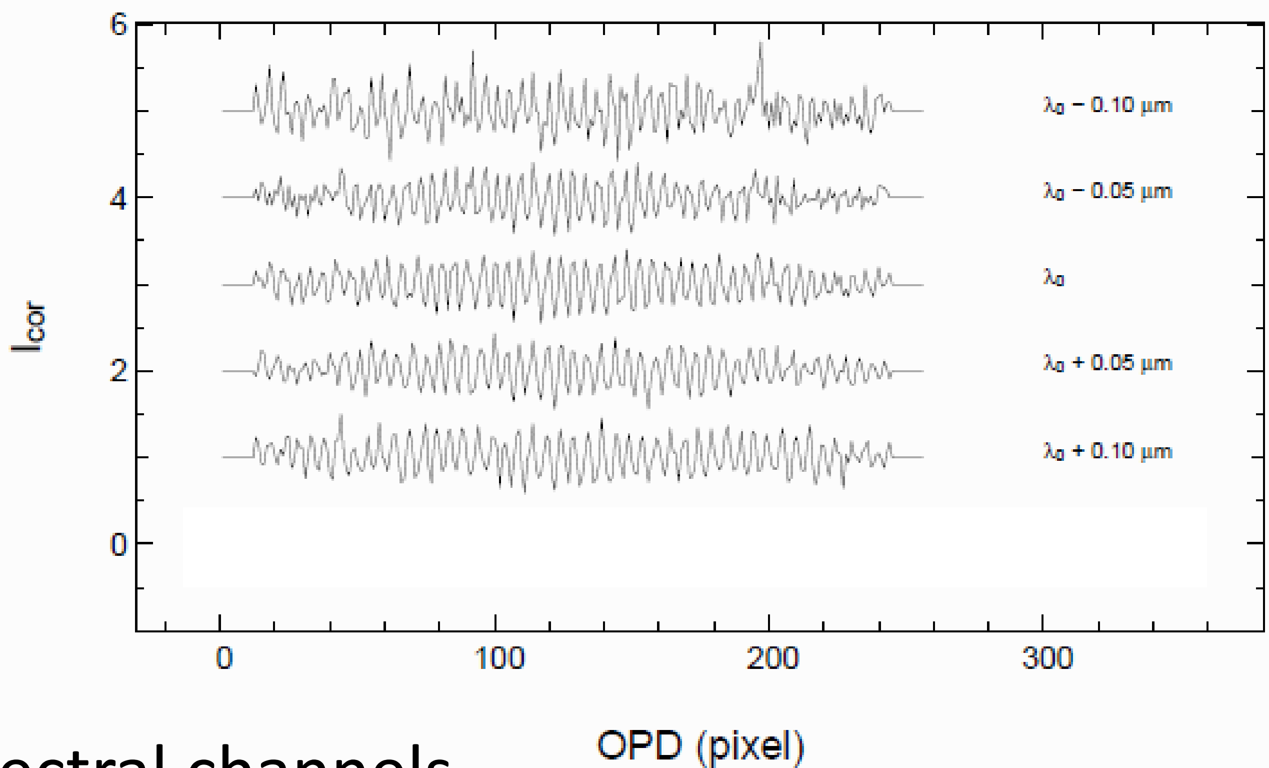

- 5 spectral channels
  - Each channel produces its own fringes
  - Minimal change to existing software (each channel can be reduced via standard DRS)

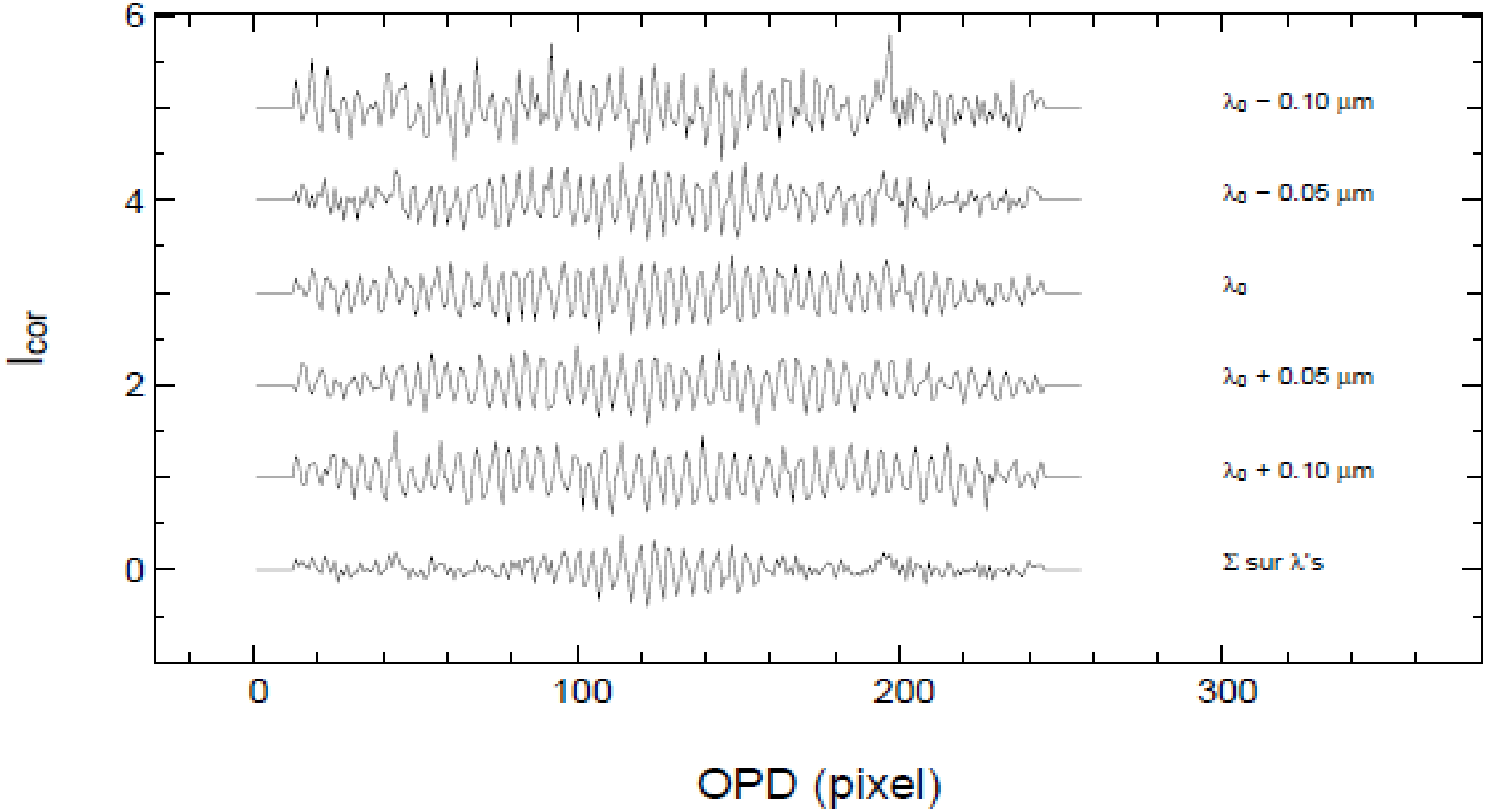

– Take sum of spectral channels and track it within the acquisition window

Differential measurable quantities

- Visibility
- Phase

Simultaneous observations

Affected by same systematic errors

Insensitive to piston

Self-calibrating

Differential Phase

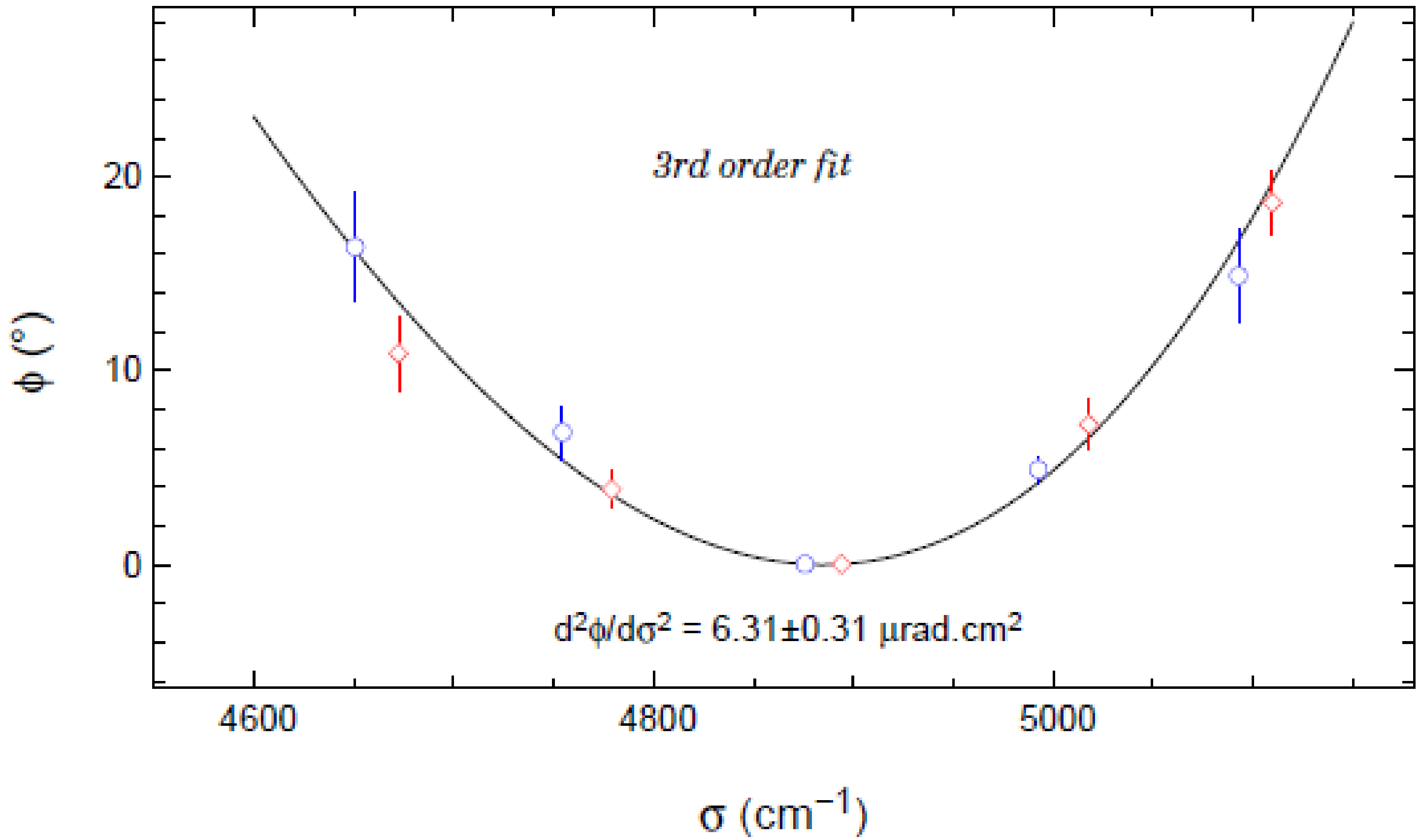

Applications

- Binaries
  - Rapid measurement
  - High precision
  - Minimal calibration
  - High throughput
- VLTI/AMBER
  - Able to detect binary and measure separation vector of Θ Orionis C using wavelength differential-visibility and closure phase modulations

No on-sky fringes for FLUOR spectral dispersion mode yet.....but later this year.

on-sky fringes image

Loading...

Special thanks to Antoine Merand, Hal McAlister, and Vincent du Foresto

References

1. ***Phdthesis* (M'erand2005)**
   Mérand, A.
   Étude à haute résolution spatiale des Céphéides
   l'Université Denis Diderot - Paris VII, **2005**
2. ***Inproceedings* (2006SPIE.6268E..46M)**
   Mérand, A.; Coudé du Foresto, V.; Kellerer, A.; ten Brummelaar, T.; Reess, J.-M. & Ziegler, D.
   CHARA/FLUOR updates and performance
   Society of Photo-Optical Instrumentation Engineers (SPIE) Conference Series, **2006***, 6268*
3. ***Article* (Kraus2009)**
   Kraus, S.; Weigelt, G.; Balega, Y. Y.; Docobo, J. A.; Hofmann, K.-H.; Preibisch, T.; Schertl, D.; Tamazian, V. S.; Driebe, T.; Ohnaka, K.; Petrov, R.; Schöller, M. & Smith, M.
   Tracing the young massive high-eccentricity binary system thetas1Orionis C through periastron passage
   aap, **2009***, 497*, 195-207
4. Hal McAlister’s ASTR 8500 notes
5. http://www.lesia.obspm.fr/astro/interfero/pages/fluor_english.html
6. http://www.ngawhetu.com/Resources/StellarRadiation/index10.html

VLTI/AMBER

S. Kraus et. al.

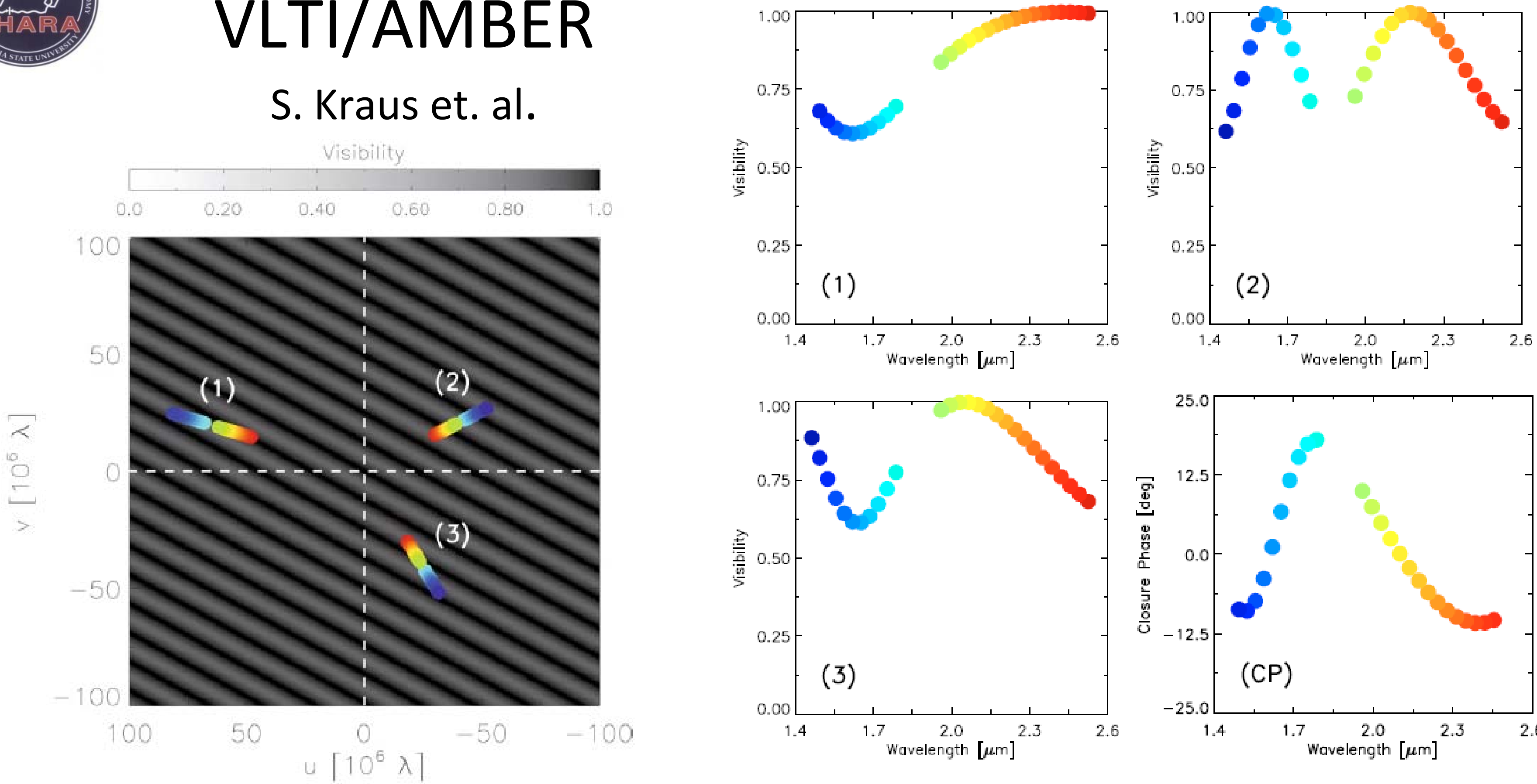

Fig. 3. Illustration of the basic principle of fitting binary parameters using wavelength-differential interferometric observables. *Left*: the VLTI/AMBER 3-telescope interferometer measures the interferometric observables in various spectral channels from 1.4 to 2.4 μm (as indicated by the color of the dots) and towards three different position angles, probing different regions in the two-dimensional Fourier spectrum of the source brightness distribution. The figure shows the visibility spectrum for a binary with ρ = 19.07 mas and Θ = 241.2° (as inferred for θ^1Ori C on 2007 Dec. 03) and the *uv*-sampling obtained with one of our AMBER observations on the same date. *Middle and right*: the visibilities and phases show a wavelength-differential modulation which is independent of the absolute calibration (see Sect. 3) and which can be fitted to analytical models.

VLTI/AMBER

S. Kraus et. al.

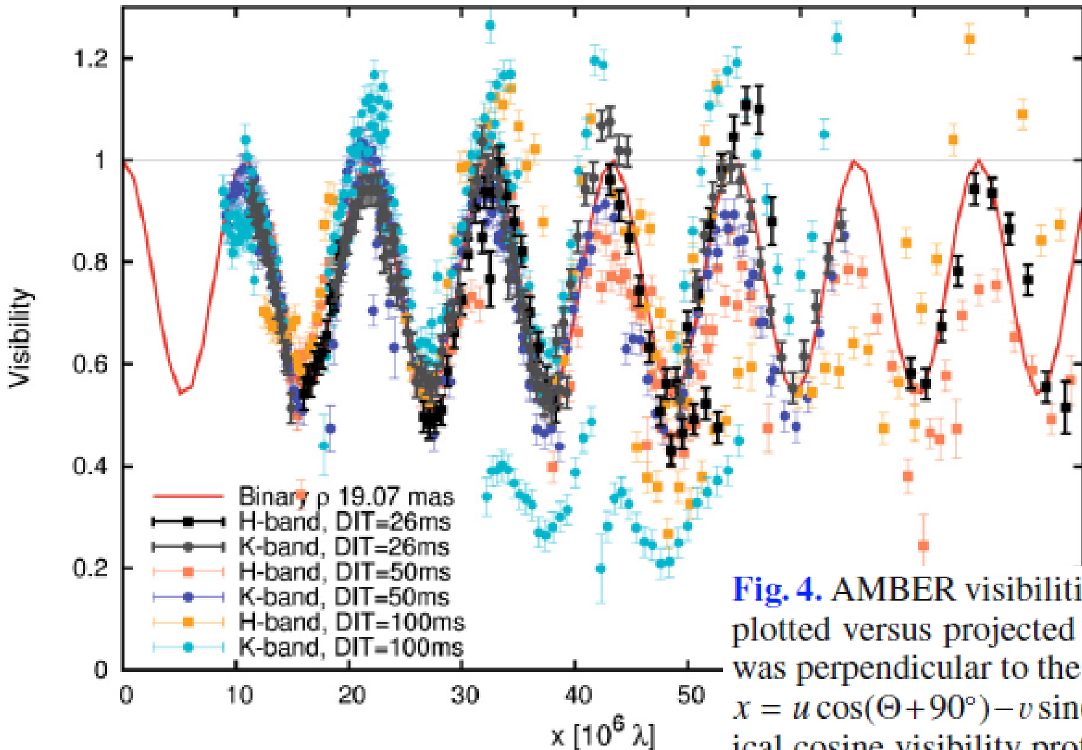

Fig. 4. AMBER visibilities measured on 2007 Dec. 03 and 2007 Dec. 05 plotted versus projected distance in the *uv*-plane (where the projection was perpendicular to the fitted binary separation vector $\Theta = 241.2°$, i.e. $x = u\cos(\Theta+90°) - v\sin(\Theta+90°)$). The solid red line shows the theoretical cosine visibility profile for a binary star with separation 19.07 mas and intensity ratio 0.30. As indicated by the strong visibility offsets, which particularly occur at high spatial frequencies, the absolute calibration is sometimes rather poor, reflecting the changing atmospheric conditions during these nights. It can also be seen that this calibration bias is particularly important for long DITs (50 ms, 100 ms), while it is nearly negligible for short DITs (26 ms, grey & black points). As expected, the spectral dependence of the visibility is not affected by these calibration uncertainties.